



Letter

Dynamics of 1D mass–spring system with a negative stiffness spring realized by magnets: Theoretical and experimental study



Akintoye Olumide Oyelade, Ziwei Wang, Gengkai Hu*

School of Aerospace Engineering, Beijing Institute of Technology, Beijing 100081, China

HIGHLIGHTS

- The interaction between a positive and negative springs in a mass–spring system is experimented, anti–phase movement is observed, confirming the analytical solution.
- We further showed the dynamics of the system containing negative stiffness (NS) spring could also be derived from Hamilton's principle.

ARTICLE INFO

Article history:

Received 6 November 2016

Accepted 29 November 2016

Available online 23 January 2017

*This article belongs to the Solid Mechanics

Keywords:

Negative stiffness

Magnets

Interaction

ABSTRACT

Realization of negative stiffness (NS) in damping low frequency acoustic and mechanical vibration is relevant in engineering applications. In this work, assemblage of two repelling magnets was used to produce negative magnetic spring (NMS). A mass–spring system with NMS is experimented where the free and forced vibrations of the system are examined. The anti–phase movement is observed due to the presence of proposed NMS, confirming the analytical solution. We further showed the dynamics of the system containing NS spring could also be derived from Hamilton's principle.

© 2017 The Authors. Published by Elsevier Ltd on behalf of The Chinese Society of Theoretical and Applied Mechanics.

This is an open access article under the CC BY–NC–ND license (<http://creativecommons.org/licenses/by-nc-nd/4.0/>).

Negative stiffness (NS) material and behavior are naturally unfamiliar to engineer, having a material assisting in deformation under load is imaginary. This unique property is however of interest to researchers [1–5], hoping to have radical technological innovations in the coming future. The idea of negative constitutive property will continue to be an academic paradox until we have sufficient analysis and experimental verification of these concepts. Though NS is unstable without constraint, its usefulness with other materials has resulted in a paradigm shift in engineering design. The NS story is no longer of instability rather a useful way to improve the performance of materials and structures. For examples in acoustic metamaterials, Lee et al. [6] presented experimental and theoretical results on a membrane–type acoustic metamaterial that exhibits a negative effective modulus in a frequency range of 0–450 Hz, which may find application in low frequency acoustic isolation and negative refraction. Another usefulness is found in an energy harvester mechanism, where a mechanical oscillator seizes and stores energy at high energy orbit vibration which results in an increased power harvesting output [7,8]. There are three broad ways to obtain NS. The first one is negative stiffness element due

to its instability that can survive within a surrounding positive stiffness matrix [9–11]. The second one is to produce NS with mechanical springs in different configurations, for example two inclined springs [12–15], inclined Euler beam [16,17], and compressed springs [18]. And the third one is using magnets in proper configurations to produce negative restoring force. Magnets are placed either in attracting manner with a mechanical spring in between [19,20], or in repelling way to produce NS [21–23]. Though NS has growing interests in engineering field, achieving sufficient condition for its stability in materials is a requirement before it can be applied. To avoid failure of designs, theoretical bounds on the effective properties of linear elastic inhomogeneous solids containing NS and discrete system with NS have been proven [24–27]. This serves as guide in tailoring the NS appropriately to achieve the desired objectives in structure. Though NS elements are available and designed in prototype for low frequency vibration isolation, their interaction with positive springs and dynamics of a mass–spring system with negative stiffness element are not addressed, particularly from experimental point of view.

In this paper, we focus on dynamics of a mass–spring system with a NS element realized by magnets connected in a repelling fashion. Previously, the use of magnets in producing NS has been with one degree of freedom instead of two, to model NS spring. We here propose experimentally a negative magnetic spring (NMS)

* Corresponding author.

E-mail address: hugeng@bit.edu.cn (G. Hu).

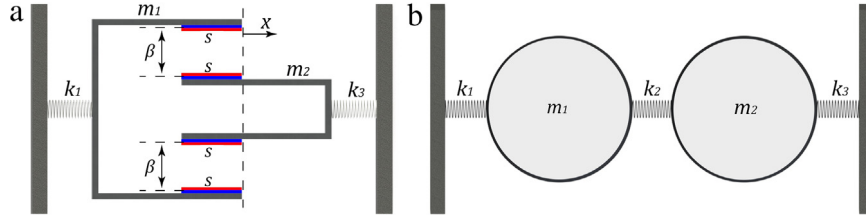


Fig. 1. (Color online) System with an NMS. (a) Its built-up, NMS containing four magnets, two magnets connected to mass 1 and the other two magnets are attached to mass 2; (b) its mass and spring idealization.

that is used within positive stiffness springs, their interaction will be examined. The NMS obtained is subjected to free and forced harmonic vibrations to determine its dynamic response and its interaction with the surrounding positive stiffness spring. Finally we further show from energy principle that the total potential energy of the system containing negative stiffness is always positive, as having been shown for a system with negative mass [28]. We should also mention that Pasternak et al. [29] have studied three springs system with a negative linear spring in series under free vibration without experiment validation.

The designed NMS is depicted in Fig. 1. The NMS is made up four identical magnets, two magnets are connected to the mass m_2 and the other two magnets are fixed at the opposing side temporarily. The analytical expression for the force interaction between two magnets is proposed by Akoun and Yonnet [30]. For our model, the force can be calculated as

$$F = -\frac{J^2}{2\pi\mu_0} \sum_{i=0}^1 \sum_{j=0}^1 \sum_{k=0}^1 \sum_{l=0}^1 \sum_{p=0}^1 \sum_{q=0}^1 (-1)^{i+j+k+l+p+q} \times \Phi(U_{ij}, V_{kl}, W_{pq}, r), \quad (1)$$

$$\Phi = 0.5(V_{kl}^2 - W_{pq}^2) \ln(r - U_{ij}) + U_{ij}V_{kl} \ln(r - V_{kl}) + V_{kl}W_{pq} \arctan\left(\frac{U_{ij}V_{kl}}{rW_{pq}}\right) + 0.5rU_{ij},$$

where

$$U_{ij} = x + (-1)^j a - (-1)^i a, \\ V_{kl} = (-1)^l b - (-1)^k b, \\ W_{pq} = \beta + (-1)^q c - (-1)^p c, \\ r = \sqrt{U_{ij}^2 + V_{kl}^2 + W_{pq}^2}. \quad (2)$$

NS stiffness between the mass and outer magnets along X direction gives

$$K_x = \frac{J^2}{2\pi\mu_0} \sum_{i=0}^1 \sum_{j=0}^1 \sum_{k=0}^1 \sum_{l=0}^1 \sum_{p=0}^1 \sum_{q=0}^1 (-1)^{i+j+k+l+p+q} \times (r + V_{kl} \ln(r - V_{kl})). \quad (3)$$

In these equations, J is the residual flux density of the permanent magnet, μ_0 is the permeability of vacuum. Rare earth magnet of neodymium iron boron model, grade N35 with a residual flux density of 1.21 T, and a relative permeability of 1.023 is used for the experiments. And the magnet of dimension size $20 \text{ mm} \times 10 \text{ mm} \times 2 \text{ mm}$ (a, b, c) is used. The distance between the magnets β is a parameter to be examined. Verification of the analytical equation for the force displacement is done through experiment as shown in Fig. 2. A laboratory scale experimental rig was designed and built to measure the force displacement relationship of moving mass 2 and temporary fixed mass 1. Magnets of the same size are used for the inner and outer positions as depicted Fig. 2(b).

The rigid plastic member with the mass 1 is fixed on the balance scale and the scale is set to zero. Plastic member is used to eliminate the effect of magnets on the rigid member. The electronic scale surface is made of aluminum which removes any interference with

magnets. The plane of the loop containing another two magnets with opposing polarizations is then hanged down vertically at the position when $x = -20 \text{ mm}$. The inner magnets are located in such a way that its magnetization direction is same as that of the outer magnets. Readjusting the height of the rig downwards gives the range of repelling force of the magnet in terms of displacement.

Figure 3(a) shows the force and displacement characteristics of the magnets for different values of β as the upper holder moves down along the x axis. Experimental measurements of the magnetic force with displacement for different magnet spacing were carried out, which confirmed the analytical method. Therefore we can plot the stiffness as function of displacement based on analytical formula, as shown in Fig. 3(b). First, we see that the smaller the distance β between the outer magnets (mass 1) and inner magnets (mass 2), the greater the force. Second, it is observed that the minimum stiffness value appears when the relative displacement of the masses is zero, and where the total restoring magnetic force of the magnets is zero. At this unique position the mass is in equilibrium due to symmetry of the repulsive forces in between the magnet. Far away from the unique position, the stiffness is positive as can be seen in both figures. When the distance β is wide the force acting on the mass 2 is small, thus a little resistance is developed for mass 1 to enter negative stiffness region. This produces small region of negative stiffness. In contrast, when the force is large (small distance β), the mass 1 acts as positive stiffness for a longer displacement before entering negative region. The equilibrium position is taken as our origin for the analysis and experiments. Though NMS exhibits strong nonlinear characteristics along displacement x , but we shall keep vibration amplitude small in order to approximately assume the linearity of the NMS.

For the NMS to act perfectly as mechanical spring in series, we consider a simple two oscillators system shown in Fig. 1(a) with its equivalent model in Fig. 1(b). Experimental setup for free and forced vibrations is given in Fig. 4(a) and (b) respectively.

Using Newton's second law, the governing equations as it was previously published [29] give

$$m_1 \ddot{x}_1 = -k_1 x_1 + k_2 (x_2 - x_1), \quad (4)$$

$$m_2 \ddot{x}_2 = k_2 (x_1 - x_2) - k_3 x_2, \quad (5)$$

where x_i ($i = 1, 2$) is the displacement of the mass m_i and dots denote differentiation with respect to time. Firstly let us consider the free vibration case of the system. Stability of a continuous material requires that the effective stiffness of the springs is greater than zero $k_{\text{eff}} = (1/k_1 + 1/k_2 + 1/k_3)^{-1} > 0$ and the stiffness matrix should be positive definite that is $k_1 + k_2 > 0$ and $k_1 k_2 + k_1 k_3 + k_2 k_3 > 0$ simultaneously [29]. The latter condition is more stringent than the former. Hence, the choice for stiffness should be guided by the latter condition for stability. For our experimental model, we use $m_1 = 174 \text{ g}$, $m_2 = 56 \text{ g}$, $k_1 = k_3 = 124 \text{ N/m}$, and k_2 depends on the distance β of the magnets. Air track used by Yao et al. [31] was used in this experiment where contact friction between the masses and the track is reduced

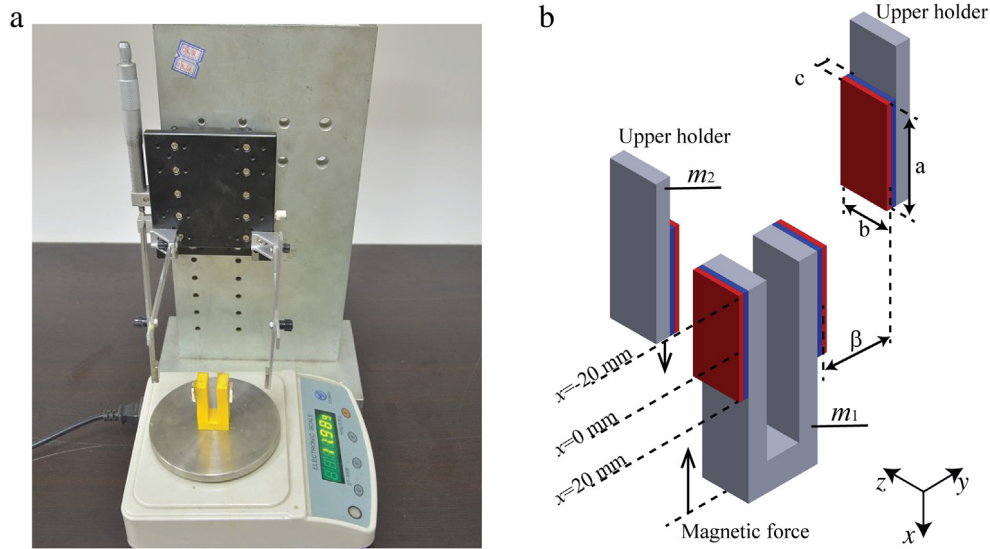


Fig. 2. (Color online) (a) Experimental setup showing the two magnets holders attached to lower and upper holders; (b) measurement principle illustration.

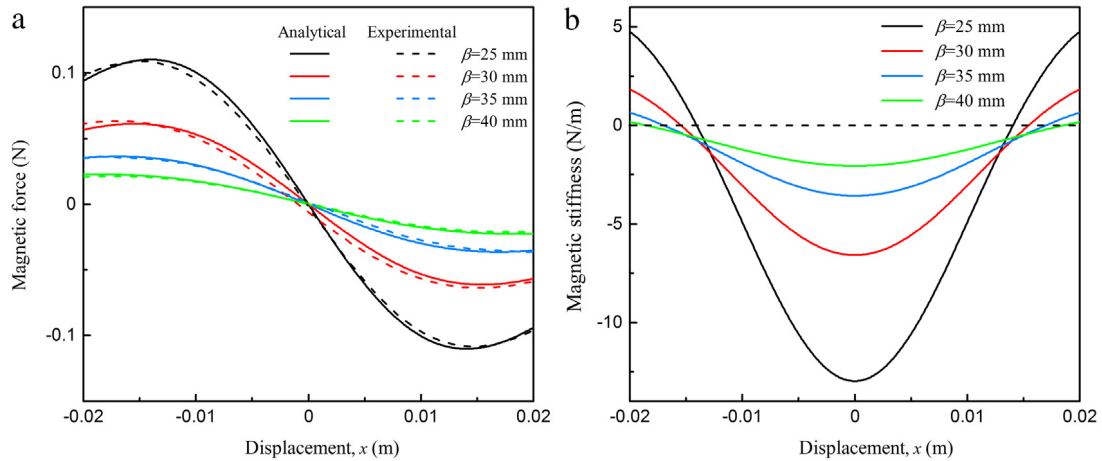


Fig. 3. (Color online) (a) Analytical and experimental magnetic force as function of displacement, (b) analytical magnetic spring stiffness.

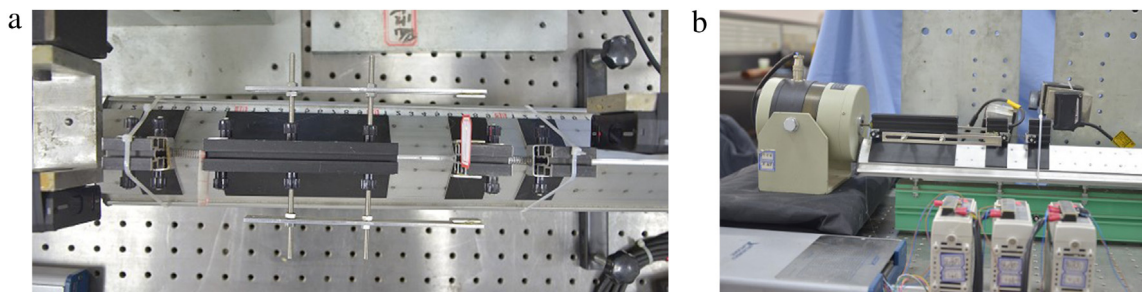


Fig. 4. (Color online) Experimental setup for two oscillators connected with NMS. (a) Free vibration, (b) forced vibration.

significantly. In the experiment, we initially displace the mass 1 from its equilibrium position and then relax this displacement, inducing a free vibration in the system. Based on the different initial conditions we determined the trajectories of the two masses as function of time, which are shown in Fig. 5. Since we maintained the NS value below the critical value, the oscillators' movement is stable. The NMS modeled the linear mechanical springs for the different spacing of magnets. In particular, from Fig. 5, the movements of the two oscillators both for the experiment

and analytical agree closely with each other. Oscillator 2 moves in anti-phase in relation to oscillator 1. The anti-phase movement of oscillator 2 due to stored energy in NMS is hereby displayed in the experiment. Instability was observed when the NS critical value is exceeded making the equilibrium position unattainable experimentally. Instead the masses separate and move to the nearest equilibrium state (positive stiffness).

Next, let us consider a situation when oscillator 1 is subjected to a forced harmonic displacement loading of $x_1 = \bar{x}_1 \cos \omega t$, then

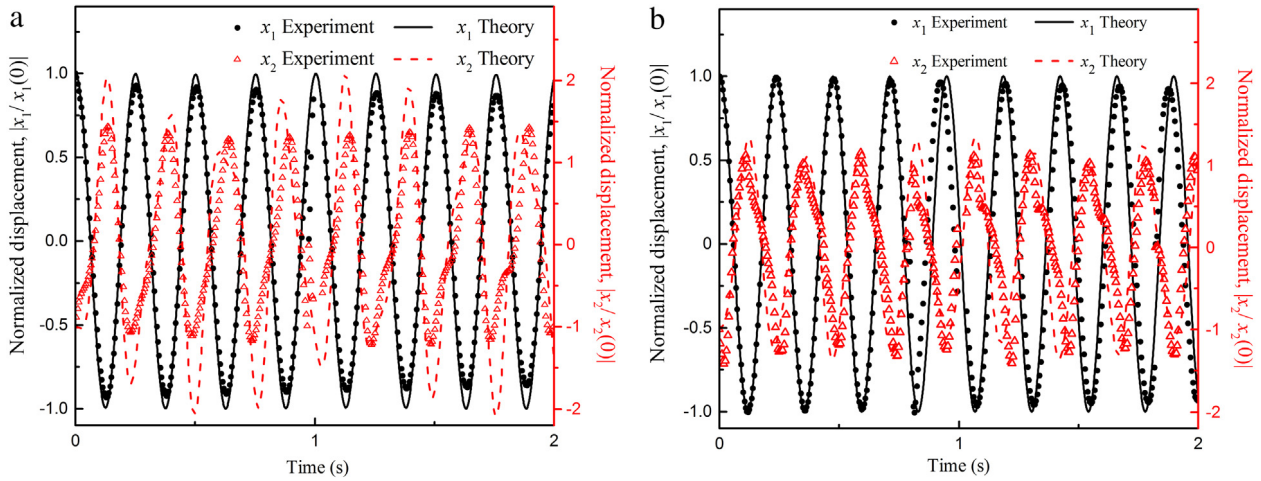


Fig. 5. (Color online) Normalized amplitude–time diagram of the systems under free vibration. (a) β equals 25 mm ($k_2 = -13$ N/m) with initial condition, $x_1(0) = 4.2$, $x_2(0) = -0.5$. (b) β equals 40 mm ($k_2 = -2.0$ N/m) with initial condition $x_1(0) = 2.9$, $x_2(0) = -0.1$. All experiments and simulations with $\dot{x}_1(0) = 0$, $\dot{x}_2(0) = 0$.

we obtain the solution for Eq. (5) as

$$\bar{x}_2 = \frac{\delta}{\omega_n^2 - \omega^2} \bar{x}_1, \quad (6)$$

where $\omega_n^2 = (k_2 + k_3)/m_2$ and $\delta = k_2/m_2$. Dynamic stability of an elastic system is ensured by real and positive eigenvalue of the problem that is $\omega_n^2 \geq 0$. Figure 6 shows the forced harmonic loading and displacement response of oscillator 2 for both experiment and theory. To cater for the difference in initial amplitude of the experimental data, we enforced the experimental initial condition to get new theoretical total response of the oscillator 2, plotted with blue dash dot line in Fig. 6. Better agreement with experiment is found if the initial displacement of the oscillator is considered. It is necessary to examine the importance of the role the NS plays in the system during forced vibration. We observed out of phase deformation of oscillator 2 due to NMS presence in the matrix, it tends to assist rather than resist deformation as a result of internally stored energy [1]. All this property can well be predicted by setting the negative value of magnetic spring, and it agrees with experiment as well.

In view of theoretical physics, magnetic spring releases some of its stored energy when the system is disturbed and work is done on the environment. It is in this manner that NS systems violate the conditions for thermodynamic. However, the energy stored and released during perturbation is harnessed in damping the response of the oscillator. This phenomenon is observed in the experimental testing in delayed response as NS increases; when energy is put into the system, the stored energy is released into the system by first neutralizing the perturbation energy on the oscillator 2, thereafter propelling it in the opposite direction. As the stored energy increases in the system, the displacement response of the oscillator in opposite direction tends to increase further.

It is instructive to consider the energy of the system with the NMS. Since we are considering thermodynamic state of a system undergoing loading, the Gibbs' theorem guarantees a stable equilibrium. Therefore, considering our free vibration loading case, it is reasonable to approximate the total energy Π of our discrete system, as the summation of the internal energies of each of its parts.

$$\Pi = \sum_{i=1}^n \Pi_i. \quad (7)$$

Energy interaction between two magnets is given by Akoun et al. [30]. For our magnets configuration, the energy can be written as

$$\begin{aligned} \Lambda &= \frac{J^2}{2\pi\mu_0} \sum_{i=0}^1 \sum_{j=0}^1 \sum_{k=0}^1 \sum_{l=0}^1 \sum_{p=0}^1 \sum_{q=0}^1 (-1)^{i+j+k+l+p+q} \\ &\quad \times \Gamma(U_{ij}, V_{kl}, W_{pq}, r), \\ \Gamma &= \frac{U_{ij}}{2} (V_{kl}^2 - W_{pq}^2) \ln(r - U_{ij}) + \frac{V_{kl}}{2} (U_{ij}^2 - W_{pq}^2) \ln(r - V_{kl}) \\ &\quad + U_{ij} V_{kl} W_{pq} \arctan\left(\frac{U_{ij} V_{kl}}{r W_{pq}}\right) + \frac{r}{6} (U_{ij}^2 + V_{kl}^2 - 2W_{pq}^2). \end{aligned} \quad (8)$$

The variables are the same as in Eq. (2). The total kinetic and potential energies of the system can be defined as

$$\begin{aligned} T &= \frac{1}{2} m_1 \dot{x}_1^2 + \frac{1}{2} m_2 \dot{x}_2^2, \\ \Pi &= \frac{1}{2} k_1 x_1^2 + \Lambda (x_2 - x_1) + \frac{1}{2} k_3 x_2^2. \end{aligned} \quad (9)$$

Introducing the Lagrangian L gives

$$L = \frac{1}{2} m_1 \dot{x}_1^2 + \frac{1}{2} m_2 \dot{x}_2^2 - \frac{1}{2} k_1 x_1^2 - \Lambda (x_2 - x_1) - \frac{1}{2} k_3 x_2^2, \quad (10)$$

where \dot{x}_i is the velocity of the m_i . The equation of motion then becomes

$$\frac{d}{dt} \left(\frac{\partial L}{\partial \dot{x}} \right) - \frac{\partial L}{\partial X} = 0, \quad (11)$$

$$m_1 \ddot{x}_1 + k_1 x_1 - k_2 (x_2 - x_1) = 0, \quad (12)$$

$$m_2 \ddot{x}_2 + k_3 x_2 + k_2 (x_2 - x_1) = 0. \quad (13)$$

Considering the forced harmonic loading case,

$$T = \frac{1}{2} m_2 \dot{x}_2^2, \quad (14)$$

$$\Pi = \Lambda (x_2 - x_1) + \frac{1}{2} k_3 x_2^2,$$

$$L = \frac{1}{2} m_2 \dot{x}_2^2 - \Lambda (x_2 - x_1) - \frac{1}{2} k_3 x_2^2. \quad (15)$$

The equation of motion then becomes

$$m_2 \ddot{x}_2 + k_2 (x_2 - x_1) + k_3 x_2 = 0. \quad (16)$$

From Eq. (10), Λ is the stored energy of the magnets which is positive. Eqs. (12), (13) and (16) derived based on Hamilton's energy principle are the same as Eqs. (4) and (5) respectively based on Newton's second law. Therefore, in terms of energy equation for NS spring mass systems, inverting the sign of the stiffness without taking note of anti-phase displacement of next oscillator will result

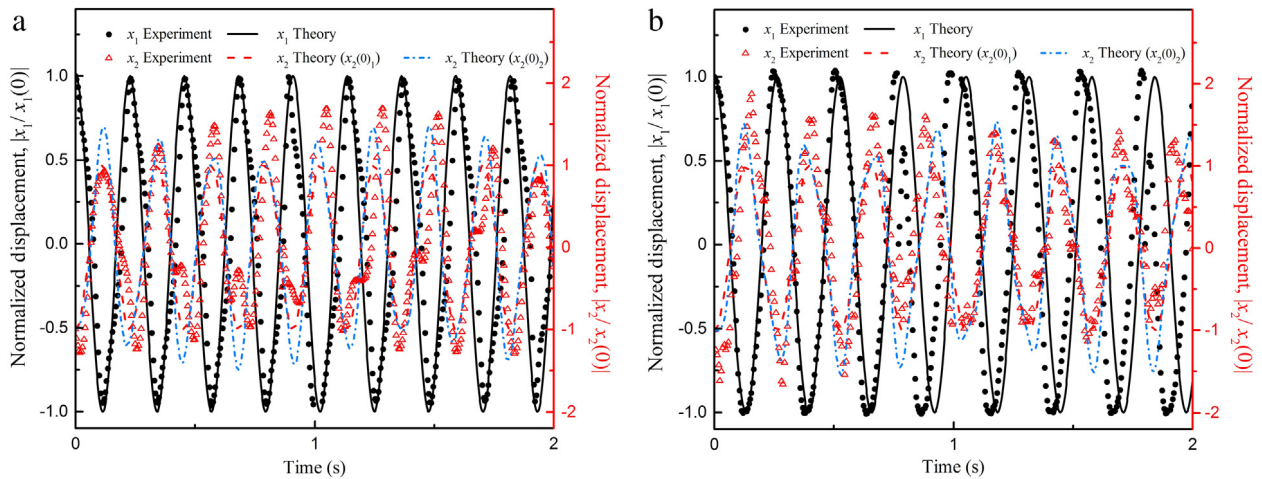


Fig. 6. (Color online) Experiment and theory under dynamic loading. (a) β equals 25 mm ($k_2 = -13$ N/m) with frequency $\omega = 4.4$ Hz with initial condition $x_1(0) = -0.14$, $x_2(0)_1 = 0$, $x_2(0)_2 = -0.14$, displayed as black, red and pink, respectively. (b) β equals 40 mm ($k_2 = -2.0$ N/m) with frequency $\omega = 3.8$ Hz with initial condition $x_1(0) = -0.01$, $x_2(0)_1 = 0$, $x_2(0)_2 = -0.01$.

in negative energy which does not characterize the energy function of the system. In the alternative, the equation containing stored energy at the initial configuration should be used. Furthermore the NMS did not violate the law of thermodynamics because the total potential energy from the derivation is positive definite for both static and dynamic loading, as demonstrated by Zhou et al. [28] for a system with negative mass.

In this work, we have demonstrated through experiment the possibility of having NS within a positive matrix without buckling or snap through of member. The boundary constraints on the system allowed the system admit NS value and NS is set within the allowable range to make for overall stability. Under dynamic loading, NMS behaves as a linear mechanical spring with anti-phase movement. Admissibility of NS without violating the law of thermodynamics is proved. This will pave way for new material design in composite engineering where theory has recognized that NS behavior can improve damping property of the material.

Acknowledgments

This work was supported by the National Natural Science Foundation of China (11472044, 11221202, 11632003, 11521062) and the 111 Project (B160030).

References

- [1] R.S. Lakes, Extreme damping in compliant composites with a negative-stiffness phase, *Phil. Mag. Lett.* 81 (2001) 95–100.
- [2] R.S. Lakes, T. Lee, A. Bersie, et al., Extreme damping in composite materials with negative-stiffness inclusions, *Nature* 410 (2001) 565–567.
- [3] Y.C. Wang, M. Ludwigson, R.S. Lakes, Deformation of extreme viscoelastic metals and composites, *Mater. Sci. Eng. A* 370 (2004) 41–49.
- [4] T. Jaglinski, D. Stone, R.S. Lakes, Internal friction study of a composite with a negative stiffness constituent, *J. Mater. Res.* 20 (2005) 2523–2533.
- [5] Y.C. Wang, R.S. Lakes, Stable extremely-high-damping discrete viscoelastic systems due to negative stiffness elements, *Appl. Phys. Lett.* 84 (2004) 4451.
- [6] S.H. Lee, C.M. Park, Y.M. Seo, et al., Acoustic metamaterial with negative density, *Phys. Lett. Sect. A Gen. At. Solid State Phys.* 373 (2009) 4464–4469.
- [7] R.L. Harnie, M. Thota, K.W. Wang, Bistable energy harvesting enhancement with an auxiliary linear oscillator, *Smart Mater. Struct.* 22 (2013) 125028.
- [8] R.L. Harnie, K.W. Wang, A review of the recent research on vibration energy harvesting via bistable systems, *Smart Mater. Struct.* 22 (2013) 023001.
- [9] H.W. Yap, R.S. Lakes, R.W. Carpick, Negative stiffness and enhanced damping of individual multiwalled carbon nanotubes, *Phys. Rev. B - Condens. Matter Mater. Phys.* 77 (2008) 045423.
- [10] L. Dong, D.S. Stone, R.S. Lakes, Extreme anelastic responses in $Zn_{80}Al_{20}$ matrix composite materials containing $BaTiO_3$ inclusion, *Scr. Mater.* 65 (2011) 288–291.
- [11] T. Jaglinski, P. Frascione, B. Moore, et al., Internal friction due to negative stiffness in the indium–thallium martensitic phase transformation, *Phil. Mag.* 86 (2006) 4285–4303.
- [12] A. Carrella, M.J. Brennan, I. Kovacic, et al., On the force transmissibility of a vibration isolator with quasi-zero-stiffness, *J. Sound Vib.* 322 (2009) 707–717.
- [13] I. Kovacic, M.J. Brennan, T.P. Waters, A study of a nonlinear vibration isolator with a quasi-zero stiffness characteristic, *J. Sound Vib.* 315 (2008) 700–711.
- [14] T.D. Le, K.K. Ahn, A vibration isolation system in low frequency excitation region using negative stiffness structure for vehicle seat, *J. Sound Vib.* 330 (2011) 6311–6335.
- [15] L.T. Danh, K.K. Ahn, Active pneumatic vibration isolation system using negative stiffness structures for a vehicle seat, *J. Sound Vib.* 333 (2014) 1245–1268.
- [16] X. Huang, X. Liu, J. Sun, et al., Vibration isolation characteristics of a nonlinear isolator using Euler buckled beam as negative stiffness corrector: A theoretical and experimental study, *J. Sound Vib.* 333 (2014) 1132–1148.
- [17] X. Liu, X. Huang, H. Hua, On the characteristics of a quasi-zero stiffness isolator using Euler buckled beam as negative stiffness corrector, *J. Sound Vib.* 332 (2013) 3359–3376.
- [18] J. Yang, Y.P. Xiong, J.T. Xing, Dynamics and power flow behavior of a nonlinear vibration isolation system with a negative stiffness mechanism, *J. Sound Vib.* 332 (2013) 167–183.
- [19] A. Carrella, M.J. Brennan, T. Waters, et al., On the design of a high-static-low-dynamic stiffness isolator using linear mechanical springs and magnets, *J. Sound Vib.* 315 (2008) 712–720.
- [20] N. Zhou, K. Liu, A tunable high-static-low-dynamic stiffness vibration isolator, *J. Sound Vib.* 329 (2010) 1254–1273.
- [21] Q. Li, Y. Zhu, D. Xu, et al., A negative stiffness vibration isolator using magnetic spring combined with rubber membrane, *J. Mech. Sci. Technol.* 27 (2013) 813–824.
- [22] R. Ravaud, G. Lemarquand, V. Lemarquand, Halbach structures for permanent magnets bearings, *Prog. Electromagn. Res. M* 14 (2010) 263–277.
- [23] W. Wu, X. Chen, Y. Shan, Analysis and experiment of a vibration isolator using a novel magnetic spring with negative stiffness, *J. Sound Vib.* 333 (2014) 2958–2970.
- [24] D.M. Kochmann, Stability criteria for continuous and discrete elastic composites and the influence of geometry on the stability of a negative-stiffness phase, *Phys. Status Solidi Basic Res.* 249 (2012) 1399–1411.
- [25] S. Xinchun, R.S. Lakes, Stability of elastic material with negative stiffness and negative Poisson's ratio, *Phys. Status Solidi Basic Res.* 244 (2007) 1008–1026.
- [26] Y.C. Wang, R. Lakes, Stability of negative stiffness viscoelastic systems, *Q. Appl. Math.* 63 (2004) 34–55.
- [27] D.M. Kochmann, W.J. Drugan, Analytical stability conditions for elastic composite materials with a non-positive-definite phase, *Proc. R. Soc. A Math. Phys. Eng. Sci.* 468 (2012) 2230–2254.
- [28] J. Zhou, Y. Cheng, H. Zhang, et al., Experimental study on interaction between a positive mass and a negative effective mass through a mass–spring system, *Theor. Appl. Mech. Lett.* 5 (2015) 196.
- [29] E. Pasternak, A.V. Dyskin, G. Sevel, Chains of oscillators with negative stiffness elements, *J. Sound Vib.* 333 (2014) 6676–6687.
- [30] G. Akoun, J.P. Yonnet, 3D analytical calculation of the forces exerted between two cuboidal magnets, *IEEE Trans. Magn.* 20 (1984) 1962–1964.
- [31] S. Yao, X. Zhou, G. Hu, Experimental study on negative effective mass in a 1D mass–spring system, *New J. Phys.* 10 (2008) 043020.